

Chapter 1

Solvation effects of ions and ionic surfactants in polar fluids

Akira Onuki

Department of Physics, Kyoto University, Kyoto 606-8502, Japan

A Ginzburg-Landau theory is presented on polar binary mixtures containing ions. It takes account of electrostatic, solvation, image, and amphiphilic interactions among the ions and the solvent molecules. The ion distributions and the electric potential are calculated around an interface with finite thickness in equilibrium. The surface tension is increased for hydrophilic ion pairs, but is decreased for hydrophilic and hydrophobic ion pairs. Introducing the amphiphilic interaction, we also treat ionic surfactants, which aggregate at an interface and reduce the surface tension. A mesophase with periodic composition and ion modulations emerges for sufficiently large asymmetry between the cationic and anionic solvation strengths. Also, among ions, there arise long-range attractive interactions in the Ornstein-Zernike form, which are mediated by the composition fluctuations. Under strong solvation conditions, they can dominate over the Coulomb interaction in the range shorter than the correlation length. In the presence of three ion species, the ion distribution can be very complex.

1.1. Introduction

In usual electrolyte theories, ions interact via the Coulombic potential in a fluid with a homogeneous dielectric constant ϵ . However, ϵ is strongly inhomogeneous particularly in the presence of mesoscopic structures in polar fluid mixtures (water and oil) or in polymer solutions. Furthermore, in most of the physics literature, the microscopic molecular interactions between ions and solvent molecules are not explicitly considered. Around a microscopic ion such as Na^+ or Cl^- in a polar fluid, the ion-dipole interaction gives rise to a solvation (hydration) shell composed of a number of solvent molecules (those of the more polar component for a mixture).^{1,2} The resultant solvation free energy per ion will be called the solvation chem-

ical potential and will be written as μ_{sol}^i where i represents the ion species. It is important that μ_{sol}^i strongly depends on the solvent density or the composition for binary mixtures, with its typical values much larger than the thermal energy $k_B T$. Thus the molecular interaction gives rise to the free energy density $\sum_i \mu_{\text{sol}}^i n_i$,^{3,4} where n_i ($i = 1, 2, \dots$) are the ion densities. It strongly influences phase transitions in polar fluids.

Using the linear dielectric constant ε , Born took into account the polarization around an ion to obtain his classic formula.⁵ It is the space integral of the electrostatic energy $\varepsilon(\nabla\Phi)^2/8\pi$ around the ion, where $\Phi = Z_i e/\varepsilon r$ is the potential with $Z_i e$ being the ion charge. The dominant contribution arises from the integral at small r as

$$(\mu_{\text{sol}}^i)_{\text{Born}} = Z_i^2 e^2 / 2\varepsilon R_{\text{ion}}^i = k_B T Z_i^2 \ell_B / R_{\text{ion}}^i, \quad (1.1)$$

where the lower cut-off R_{ion}^i is called the Born radius.¹ In terms of the Bjerrum length $\ell_B \equiv e^2/\varepsilon k_B T$, we can see $(\mu_{\text{sol}}^i)_{\text{Born}} > k_B T$ for $R_{\text{ion}}^i < \ell_B$. For mixtures of two fluid components, A and B, ε changes from the dielectric constant ε_B of the less polar component B to that ε_A of the more polar component A with increasing the volume fraction ϕ of the more polar component A, so the Born formula indicates strong dependence of μ_{sol}^i on ϕ . However, it is well-known that the Born formula neglects electrostriction (leading to the shell formation) and nonlinear dielectric saturation (due to strong electric field in the vicinity of an ion).

We consider a fluid-fluid interface between a polar phase α and a less polar phase β with bulk compositions ϕ_α and ϕ_β , across which there arises a difference of μ_{sol}^i because of its composition dependence:

$$\Delta\mu_{\alpha\beta}^i = \mu_{\text{sol}}^{i\beta} - \mu_{\text{sol}}^{i\alpha}, \quad (1.2)$$

where μ_{sol}^{iK} ($K = \alpha, \beta$) are the bulk values of the solvent chemical potential of species i in the two phases. In electrochemistry,^{6,7} the difference of the solvation free energies $\Delta G_{\alpha\beta}^i$ between two phases have been called the standard Gibbs transfer energy. (Since $\Delta G_{\alpha\beta}^i$ are usually measured in units of kJ per mole, dividing them by the Avogadro number gives $\Delta\mu_{\alpha\beta}^i$). It is well-known that if there are differences among $\Delta\mu_{\alpha\beta}^i$ ($i = 1, 2, \dots$), an electric double layer emerges at the interface, giving rise to an electric potential jump $\Delta\Phi = \Phi_\alpha - \Phi_\beta$, called the Galvani potential difference, across the interface in equilibrium. In particular, if there are only two species of ions ($i = 1, 2$) with charges $Z_1 e$ and $-Z_2 e$ ($Z_1 > 0$ and $Z_2 > 0$), the Galvani potential difference is expressed as^{4,6}

$$e\Delta\Phi = (\Delta\mu_{\alpha\beta}^2 - \Delta\mu_{\alpha\beta}^1)/(Z_1 + Z_2), \quad (1.3)$$

and the ion densities in the bulk two phases are related by

$$\ln \left(\frac{n_{1\alpha}}{n_{1\beta}} \right) = \ln \left(\frac{n_{2\alpha}}{n_{2\beta}} \right) = \frac{Z_1 Z_2}{Z_1 + Z_2} \left[\frac{\Delta\mu_{\alpha\beta}^1}{Z_1 k_B T} + \frac{\Delta\mu_{\alpha\beta}^2}{Z_2 k_B T} \right], \quad (1.4)$$

at sufficiently low ion densities. These relations readily follow from the continuity of the (total) ionic chemical potentials across the interface and the charge neutrality conditions in the bulk two phases. Note that $\Phi(z)$ near a thin interface changes on the scale of the Debye-Hückel screening length, κ_α^{-1} in the α phase and κ_β^{-1} in the β phase. As a result, Φ changes from Φ_α to Φ_β on the spatial scale of $\kappa_\alpha^{-1} + \kappa_\beta^{-1}$, which becomes very long as the ion densities determined by Eq.(1.4) become very small in one of the two phases.⁴ Remarkably, $\Delta\Phi$ in Eq.(1.3) is independent of the ion densities. It is typically of order $10k_B T/e$ (~ 0.1 Volt) for $\Delta\mu_{\alpha\beta}^2 \neq \Delta\mu_{\alpha\beta}^1$. It vanishes for symmetric ion pairs with $\Delta\mu_{\alpha\beta}^2 = \Delta\mu_{\alpha\beta}^1$. As Eq.(1.4) indicates, the ion densities in the two phases are very different in many cases. For example, if $\Delta\mu_{\alpha\beta}^1/k_B T = \Delta\mu_{\alpha\beta}^2/k_B T = 10$ in the monovalent case, the common ratio $n_{1\beta}/n_{1\alpha} = n_{2\beta}/n_{2\alpha}$ becomes $e^{-10} = 2.4 \times 10^{-4}$.

In the literature, data of $\Delta G_{\alpha\beta}^i$ on water-nitrobenzene at room temperatures are available,^{6,7} where the two components are strongly segregated. For aqueous mixtures with α being the water-rich phase, $\Delta G_{\alpha\beta}^i$ is positive for hydrophilic ions and negative for hydrophobic ions. For water-nitrobenzene,⁶ we have $\Delta\mu_{\alpha\beta}^i/k_B T = 13.6$ for Na^+ , 15.3 for Li^+ , 26.9 for Ca^{2+} , 11.3 for Br^- , and 7.46 for I^- as examples of hydrophilic ions, while we have $\Delta\mu_{\alpha\beta}^i/k_B T = -14.4$ for BPh_4^- (tetraphenylborate) as an example of hydrophobic ions. Thus, the solvent chemical potential $\mu_{\text{sol}}^i(\phi)$ strongly depends on the composition ϕ , as well as the dielectric constant $\varepsilon(\phi)$.

As another consequence, $\Delta\mu_{\alpha\beta}^i$ is an important parameter dramatically influencing the nucleation process in polar fluids with ions. That is, when a polar fluid in a less polar phase β is brought into a metastable state, the solvation shell around an ion can serve as a seed of a critical droplet of a more polar phase α .⁸ For water at $T = 0.6T_c \cong 390$ K, for example, $\Delta\mu_{\alpha\beta}^i/k_B T$ can be of order 50 – 100 between gaseous water (phase β) and liquid water (phase α).⁹ The nucleation barrier is much reduced in the presence of ions.

The surface tension γ of a water-air interface has been examined extensively in the literature. Theoretically, Wagner¹⁰ found that ions in water are repelled away from the interface by the image charges in air, leading to an increase of the surface tension $\Delta\gamma > 0$. Using Wagner's idea, Onsager

and Samaras¹¹ obtained the limiting law for the excess surface tension,

$$\Delta\gamma = k_B T n_w D_I [\ln(1/D_I \kappa) + E_I], \quad (1.5)$$

where $D_I = \ell_{Bw}/4$ and E_I is a dimensionless constant of order unity with the Bjerrum length $\ell_{Bw} = e^2/\varepsilon_w k_B T$ being 7\AA in room-temperature water. The above expression is valid for $\kappa_w \ell_{Bw} \ll 1$ and in the thin limit of the interface width ξ . Levin and Flores-Mena¹² argued that an ion-depletion layer is formed due to the finite size of the solvation shell radius¹ (even without the image force). In these theories the interface thickness ξ is assumed to be infinitesimal. In our recent theory,⁴ the interface is diffuse and the composition-dependent solvation interaction serves to repel hydrophilic ions away from the interface (see discussions below Eq.(2.12)). Experimentally, at not extreme dilution, the linear behavior

$$\Delta\gamma = T n_w \lambda_s \quad (1.6)$$

has been measured,^{13–15} where λ_s is the effective thickness of the ion-depletion layer. For example, $\lambda_s \sim 3\text{\AA}$ for NaCl, where the densities of Na^+ and Cl^- are $n_w/2$. For very dilute salts around 1 mM in aqueous solutions, Jones and Ray¹³ detected a small negative minimum in $\Delta\gamma$, which still remains an unsolved controversy.^{15,16} For water-oil interfaces, γ largely decreases with addition of hydrophilic and hydrophobic ions,¹⁷ while the linear law (1.6) holds for hydrophilic ion pairs. On the other hand, in the presence of surfactants, γ decreases due to excess adsorption of the surfactant molecules on an interface.¹⁸

In this chapter, we explain some fundamental solvation effects in a binary fluid mixture on the basis of our recent work.^{3,4} Similar approaches have also been proposed by other authors.^{16,19,20} We will assume that the dielectric constant in the more polar phase is twice larger than that in the less polar phase, so we will consider water-oil systems like water-nitrobenzene (the dielectric constant of nitrobenzene is about 36). In Section 2, we will present a Ginzburg-Landau approach to the molecular interactions between ions and solvent molecules. In addition to the solvation and image interactions, we will propose a free energy contribution representing the amphiphilic interaction between surfactant and solvent molecules. We may then treat ionic surfactants and counterions which have charges and aggregate at an interface reducing the surface tension. In Section 3, we will calculate the composition structure factor and the ion interaction mediated by the composition fluctuations near the critical point of the mixture. They can be strongly affected even by a small amount of ions. In particular, we

will discuss a mesophase with a charge density wave, which can appear for large solvation asymmetry between cations and anions. In Section 4, we will derive some fundamental relations on the equilibrium ion distributions and the surface tension. We will study the case of three ion species. In Section 5, we will give some numerical results on the ion distributions and the surface tension in various cases.

1.2. Ginzburg-Landau theory

1.2.1. Solvation interaction

Let us consider a polar binary mixture (water and oil) containing a small amount of salt. The volume fraction of the more polar component is written as ϕ . The other less polar component has the volume fraction $1 - \phi$. We neglect the volume fractions of the ions in this chapter. The ion densities are written as n_1, n_2, \dots . In our theory, we mostly suppose two ion species with charges $Q_1 = Z_1 e$ and $Q_2 = -Z_2 e$, but we will also treat more complex cases in the presence of three ion species. In our scheme, ϕ, n_1, n_2, \dots are smooth space-dependent variables coarse-grained on the microscopic level. We present a Ginzburg-Landau scheme, where the interface thickness ξ is supposed to be longer than the molecular size a .

The usual form of the free energy for a fluid mixture containing a small amount of ions is written as

$$F_0 = \int d\mathbf{r} \left[f_0(\phi, T) + \frac{C}{2} |\nabla\phi|^2 + \frac{\varepsilon(\phi)}{8\pi} \mathbf{E}^2 + k_B T \sum_i n_i \ln(n_i a^3) \right]. \quad (2.1)$$

As discussed in the first section, we introduce the solvation free energy,^{3,4}

$$F_{\text{sol}} = \int d\mathbf{r} \sum_i n_i \mu_{\text{sol}}^i(\phi). \quad (2.2)$$

The free energy density f_0 is dependent on ϕ and T . For low molecular-weight mixtures we may use the Bragg-Williams form,

$$f_0 = a^{-3} k_B T [\phi \ln \phi + (1 - \phi) \ln(1 - \phi) + \chi \phi(1 - \phi)]. \quad (2.3)$$

Our theory can be used also for polymer solutions and blends if we use the Flory-Huggins form for f_0 .^{18,21} We assume that the molecules of the two fluid components (the monomers for polymers) have a common volume a^3 . The χ is the interaction parameter dependent on T , whose critical value is 2 for the free energy density in Eq.(2.3). The second term in the brackets of Eq.(2.1) is the gradient part, where we will set $C = k_B T \chi / a$ in our

numerical analysis.¹⁸ The third term is the electrostatic free energy with $\mathbf{E} = -\nabla\Phi$ being the electric field. The electrostatic potential Φ satisfies

$$-\nabla \cdot \varepsilon(\phi)\nabla\Phi = 4\pi\rho, \quad (2.4)$$

where ε is the composition-dependent dielectric constant and ρ is the charge density. When there are only two species of ions, we have $\rho = Z_1en_1 - Z_2en_2$. The last term in F_0 in Eq.(2.1) is the entropic contribution valid at low ion densities.

We do not know the functional forms of $\varepsilon(\phi)$ and $\mu^i(\phi)$. We assume the linear composition dependence,

$$\varepsilon(\phi) = \varepsilon_c + \varepsilon_1\psi, \quad (2.5)$$

$$\mu_{\text{sol}}^i(\phi) = \mu_c^i - k_B T g_i \psi \quad (i = 1, 2). \quad (2.6)$$

where $\psi = \phi - \phi_c$ is the deviation from the critical composition ϕ_c . Then ε_c and μ_c^i are the critical values. We adopt these linear forms to obtain the physical consequences in the simplest manner. Empirically, ε can be approximated as a linear function of the composition in many mixtures investigated so far.^{2,22} The first term μ_c^i on the right hand side of Eq.(2.6) is an irrelevant constant when the ion numbers are conserved quantities without dissociation processes. It then follows the relation,

$$\Delta\mu_{\alpha\beta}^i = k_B T g_i \Delta\phi, \quad (2.7)$$

where $\Delta\phi = \phi_\alpha - \phi_\beta$ is the composition difference. In aqueous mixtures, the coupling constants g_i are positive for hydrophilic ions and negative for hydrophobic ions. The experimental values of the Gibbs transfer energy for water-nitrobenzene^{6,7} suggest that the values of g_i are typically of order 15 for monovalent hydrophilic ions and are even larger for multivalent ions such as Ca^{2+} or Al^{3+} . For the hydrophobic anion BPh_4^- , it is about -15 , on the other hand. The resultant solvation coupling between the ions and the composition is very strong. The Born formula in Eq.(1.1) gives $(g_i)_{\text{Born}} = Z_i^2 e^2 \varepsilon_1 / 2k_B T \varepsilon_c^2 R_{\text{ion}}^i$ near the critical point, but we do not use it because of the defect of the Born theory. We rather treat g_i as free parameters characterizing the strength of the solvation interaction.

1.2.2. Image interaction

Inhomogeneous dielectric constant ε gives rise to an image chemical potential $Z_i^2 \mu_{\text{im}}$ acting on each ion (which is proportional to the square of its charge).⁴ We then construct the free energy contribution $F_{\text{im}} =$

$\int d\mathbf{r} \sum_i \mu_{\text{im}}^i n_i$. Note that F_{im} originates from the discrete nature of ions, while the electric field Φ determined by Eq.(2.4) is produced by the smoothly coarse-grained charge density ρ . Therefore, the origin of F_{im} is different from that of the electrostatic free energy $\int d\mathbf{r} \varepsilon \mathbf{E}^2 / 8\pi$ in Eq.(2.1).

In our previous work,⁴ assuming weak or moderate spatial variations of ε , we derived the following integral form valid to first order in ε_1 ,

$$\mu_{\text{im}}(\mathbf{r}) = \int d\mathbf{r}' \nabla' I(\mathbf{r}, \mathbf{r}') \cdot \nabla' \phi(\mathbf{r}'), \quad (2.8)$$

where $\nabla' = \partial/\partial\mathbf{r}'$. If the boundary effects are neglected, the function $I(\mathbf{r}, \mathbf{r}')$ depends only on the difference $\mathbf{r} - \mathbf{r}'$ as

$$I(\mathbf{r}, \mathbf{r}') = B_0 e^{-2\kappa|\mathbf{r}-\mathbf{r}'|} / |\mathbf{r} - \mathbf{r}'|^2, \quad (2.9)$$

where $B_0 = e^2 \varepsilon_1 / 8\pi \varepsilon_c^2$ near the critical point and κ is the Debye-Hückel wave number. The factor $e^{-2\kappa|\mathbf{r}-\mathbf{r}'|}$ arises from the screening of the image potential by the other ions, so the image interaction is weakened with increasing the ion density. In particular, around a planar interface, where all the quantities vary along the z direction, it follows the following Cauchy integral form,

$$\mu_{\text{im}}(z) = k_B T A a \frac{\varepsilon_1}{\varepsilon_c} \int \frac{dz'}{\pi} \frac{e^{-2\kappa|z-z'|} d\phi(z')}{z - z' dz'}. \quad (2.10)$$

We define the coefficient A by

$$A = \pi e^2 / 4a \varepsilon_c k_B T = \pi \ell_{\text{Bc}} / 4a \quad (2.11)$$

where $\ell_{\text{Bc}} = e^2 / \varepsilon_c k_B T$ is the Bjerrum length at $\varepsilon = \varepsilon_c$. Around an interface, where κ varies significantly, κ in Eq.(2.10) may be taken as the space-dependent local value $[4\pi e^2 m(\mathbf{r}) / \varepsilon(\mathbf{r}) k_B T]^{1/2}$ or the bulk value in the more polar phase. In our previous calculations of the surface tension⁴ there was no significant difference in these two choices.

Let us consider the thin interface limit $\xi \rightarrow 0$, where we set $d\phi(z)/dz = -\Delta\phi\delta(z)$ with $\Delta\phi = \phi_\alpha - \phi_\beta$. Placing the interface at $z = 0$, we obtain $\mu_{\text{im}}(z) \propto e^{-2\kappa|z|}/z$ for $|z| \gg \xi$ in agreement with the original expression for the image potential.^{11,12} For finite ξ , μ_{im} changes from positive to negative in the interface region $|z| \lesssim \xi$. In our theory $\mu_{\text{im}}(z)$ is negative in the less polar phase β , where the ions are attracted to the interface. We should clarify the condition in which the image interaction is important. In the α region near an interface, it causes a significant ion depletion for

$Z_i^2 \mu_{\text{im}}(z)/k_B T > 1$ at $|z| \sim \xi$ where ξ is the interface thickness. From Eq.(2.10) this condition is rewritten as

$$\xi < Z_i^2 \ell_{\text{Bc}} \varepsilon_1 \Delta\phi / \varepsilon_c < \kappa_\alpha^{-1}. \quad (2.12)$$

If the two ions are both strongly hydrophilic (or if g_1 and g_2 take large positive values), we may reproduce the formula (1.6) for $\Delta\gamma$ with $D_I = aA\varepsilon_1 \Delta\phi / \pi\varepsilon_c$.⁴ For $\Delta\phi \sim 1$ and $\varepsilon_1/\varepsilon_c \sim 1$, Eq.(2.12) becomes $\xi/a < Z_i^2 A < (a\kappa_\alpha)^{-1}$, where A is defined by eq.(2.11).

For finite interface thickness ξ , hydrophilic ions are repelled from an interface also due to the solvation interaction (due to the factor $e^{g_i\phi}$ in Eqs.(4.5) and (4.6) below for $g_i > 0$). Thus, even in the absence of the image interaction, a depletion layer of hydrophilic ions can be formed and the linear behavior $\Delta\gamma \propto n_\alpha$ still follows. To draw qualitative results, the image interaction may be neglected for not very large A . See the discussions around Eqs.(1.5) and (1.6).

1.2.3. Amphiphilic interaction

In our previous work,⁴ we calculated the ion distributions around an interface for simple structureless ions, including the solvation and image interactions. However, in many important applications, ions have an amphiphilic character and are preferentially adsorbed onto an interface. Here, extending our previous theory, we calculate the ion distributions when the first ion species is a cationic surfactant. The second species constitutes anionic counterions having no amphiphilic character.

We suppose a rod-like shape of the molecules of the first species. The rod length 2ℓ is considerably longer than a . We then introduce an amphiphilic free energy,

$$F_{\text{am}} = -k_B T \int d\mathbf{r} n_1 \ln Z_{\text{am}}, \quad (2.13)$$

where Z_{am} is the partition function of a rod-like dipole with its center at the position \mathbf{r} . It is given by the following integral on the surface of a sphere with radius ℓ ,

$$Z_{\text{am}}(\mathbf{r}) = \frac{1}{4\pi} \int d\Omega \exp \left[-w_a \phi(\mathbf{r} + \ell\mathbf{u}) + w_a \phi(\mathbf{r} - \ell\mathbf{u}) \right], \quad (2.14)$$

where the rod direction is along the unit vector \mathbf{u} and $\int d\Omega$ represents the integration over the angles of \mathbf{u} . The two ends of the rod are at $\mathbf{r} + \ell\mathbf{u}$ and $\mathbf{r} - \ell\mathbf{u}$ under the influence of the solvation potentials given by

$k_B T w_a \phi(\mathbf{r} + \ell \mathbf{u})$ and $-k_B T w_a \phi(\mathbf{r} - \ell \mathbf{u})$, respectively. Our amphiphilic interaction is characterized by ℓ and w_a . When the rod length 2ℓ is longer than the interface thickness ξ , a surfactant molecule can be trapped at an interface with its hydrophilic (hydrophobic) end in the water-rich (water-poor) region. The resultant chemical potential decrease is given by

$$\epsilon_a = k_B T w_a \Delta \phi. \quad (2.15)$$

It is instructive to examine the case in which $\phi(\mathbf{r})$ varies slowly. If the expansion $\phi(\mathbf{r} + \ell \mathbf{u}) - \phi(\mathbf{r} - \ell \mathbf{u}) = 2\ell \mathbf{u} \cdot \nabla \phi + \dots$ is allowable, we obtain

$$\ln Z_{\text{am}} = \frac{2}{3} w_a^2 \ell^2 |\nabla \phi|^2 + \dots. \quad (2.16)$$

The free energy F_{am} then provides a gradient contribution, so it may be combined with the original one ($\propto C$) in the total free energy. The new gradient term is of the form $C_{\text{eff}} |\nabla \phi|^2 / 2$ with²³

$$C_{\text{eff}} = C - \frac{4}{3} k_B T w_a^2 \ell^2 n_1 = C(1 - n_1/n_{1L}). \quad (2.17)$$

We notice the presence of a Lifshitz point at $n_1 = n_{1L}$ with

$$n_{1L} = \frac{3C}{4(\ell w_a)^2 k_B T}. \quad (2.18)$$

For $n_1 > n_{1L}$, a homogeneous electrolyte solution should be unstable at a finite wave number (see Eq.(3.3)), leading to a mesophase. If $C \sim k_B T/a$, we have $a^3 n_{1L} \sim (a/\ell w_a)^2$, so n_{1L} can be very small for large $w_a \gg 1$.

The above gradient expansion is invalid around an interface far from the critical point or for $\xi \lesssim 2\ell$. We should examine the behavior of Z_{am} around a strongly segregated interface. In the one-dimensional (1D) case, where all the quantities vary along the z axis, Z_{am} in Eq.(2.14) is simplified into the following 1D integral,

$$Z_{\text{am}}(z) = \frac{1}{2\ell} \int_{-\ell}^{\ell} d\zeta \exp \left[-w_a \phi(z + \zeta) + w_a \phi(z - \zeta) \right], \quad (2.19)$$

where we have replaced $\phi(\mathbf{r} \pm \ell \mathbf{u})$ by $\phi(z \pm \zeta)$ with $\zeta = \ell u_z$. This form indicates that the adsorption should be significant for $w_a \Delta \phi = \epsilon_a/k_B T \gg 1$. We assume this condition in the thin interface limit $\xi \ll \ell$ for simplicity. The integrand in Eq.(2.19) can be large ($= e^{w_a \Delta \phi}$) only if the interface is located between $z + \zeta$ and $z - \zeta$. With the interface being placed at $z = 0$, we find

$$Z_{\text{am}} = 1 + (1 - |z|/\ell) [\cosh(w_a \Delta \phi) - 1] \quad (2.20)$$

for $|z| < \ell$, while $Z_{\text{am}} \cong 1$ for $|z| > \ell$. In the thin interface limit, we estimate the surfactant adsorption at the interface per unit area as

$$\Gamma_1 = (n_{1\alpha} + n_{1\beta})\ell[\cosh(w_a\Delta\phi) - 1]/2, \quad (2.21)$$

where the image interaction is neglected. The $n_{1\alpha}$ and $n_{1\beta}$ are the bulk surfactant densities far from the interface. As a result, the surface tension γ decreases by $2k_B T\Gamma_1$ from the Gibbs formula (see Eq.(4.25)), where the factor 2 accounts for the counterions. For $w_a\Delta\phi \gg 1$, the decrease of γ is considerable for $n_{1\alpha} \gtrsim e^{-w_a\Delta\phi}/a^2\ell$ where we assume $\gamma \sim k_B T/a^2$ without surfactant. It is worth noting that the proportionality relation $\Gamma_1 \propto n_{1\alpha} e^{\epsilon_a/k_B T}$ for dilute surfactants was first found by Traube in his experiment.²⁴

1.3. Structure factor of composition and interactions among ions in one-phase states

In our previous papers,^{3,4} we examined the structure factor $S(q) = \langle |\phi_{\mathbf{q}}|^2 \rangle$ of the composition fluctuations with wave number q in one-phase states. Here we consider a binary mixture near the critical point with a small amount of two ion species. As a generalization, we use the Flory-Huggins free energy density for f_0 in Eq.(2.1) and include the amphiphilic interaction. We shall see that the ion-solvent interaction can strongly affect the composition fluctuations and the interaction among ions. We may neglect the image interaction near the critical point.

1.3.1. Composition fluctuations and mesoscopic phase

We consider small plane-wave fluctuations with wave vector \mathbf{q} in a homogeneous one-phase state near the critical point, where the inhomogeneity in the dielectric constant may be neglected ($\epsilon = \epsilon_c$). The fluctuation contributions to F in the bilinear order are written as

$$\delta F = \sum_{\mathbf{q}} \left[\frac{1}{2} (\bar{r} + C_{\text{eff}} q^2) |\phi_{\mathbf{q}}|^2 + \frac{2\pi}{\epsilon_c q^2} |\rho_{\mathbf{q}}|^2 + k_B T \sum_{i=1,2} \left(\frac{|n_{i\mathbf{q}}|^2}{2n_i} - g_i n_{i\mathbf{q}} \phi_{\mathbf{q}}^* \right) \right], \quad (3.1)$$

where $\phi_{\mathbf{q}}$, $n_{i\mathbf{q}}$, and $\rho_{\mathbf{q}}$ are the Fourier components of $\phi(\mathbf{r})$, $n_i(\mathbf{r})$, and $\rho(\mathbf{r}) = e[Z_1 n_1(\mathbf{r}) - Z_2 n_2(\mathbf{r})]$, respectively. The image interaction is neglected. The n_i in the last term of Eq.(3.1) are the average ion densities satisfying $Z_1 n_1 = Z_2 n_2$ from the overall charge neutrality. We use the Flory-Huggins

free energy (only in this subsection) to calculate the coefficient \bar{r} as

$$\bar{r} = \frac{\partial^2 f_0}{\partial \phi^2} = \frac{k_B T}{a^3} \left[\frac{1}{N_1 \phi} + \frac{1}{N_2 (1 - \phi)} - 2\chi \right] \quad (3.2)$$

where N_1 and N_2 are the polymerization indices of the two components. The previous results^{3,4} can be obtained for $N_1 = N_2 = 1$. If the first ion species is a cationic surfactant, the coefficient of the gradient term becomes C_{eff} in Eq.(2.17), which is assumed to be positive here. We minimize δF with respect to $n_i \mathbf{q}$ to obtain the free energy change $\delta F = \sum_{\mathbf{q}} k_B T |\phi \mathbf{q}|^2 / S(q)$, where $S(q)$ is the composition structure factor. Some calculations give

$$\frac{k_B T}{S(q)} = \bar{r} - \Delta r_{\text{ion}} + C_{\text{eff}} q^2 \left[1 - \gamma_p^2 + \frac{\gamma_p^2 q^2}{\kappa^2 + q^2} \right], \quad (3.3)$$

where $\kappa = [4\pi(Z_1^2 n_1 + Z_2^2 n_2)e^2 / \epsilon_c k_B T]^{1/2}$ is the Debye-Hückel wave number and Δr_{ion} is a constant shift of \bar{r} . From Eq.(3.2) we may define the ion-induced shift of χ by

$$\begin{aligned} \chi_c^{\text{ion}} &= \Delta r_{\text{ion}} a^3 / 2k_B T \\ &= (Z_2 g_1 + Z_1 g_2)^2 a^3 n / 2(Z_1 + Z_2)^2. \end{aligned} \quad (3.4)$$

where $n = n_1 + n_2$. In our problem there appears a dimensionless parameter γ_p representing the ion asymmetry,

$$\begin{aligned} \gamma_p &= (k_B T / 4\pi C_{\text{eff}} \ell_{Bc})^{1/2} |g_1 - g_2| / (Z_1 + Z_2) \\ &= |g_1 - g_2| / [4(Z_1 + Z_2) \sqrt{\chi A (1 - n_1 / n_{iL})}], \end{aligned} \quad (3.5)$$

where $\ell_{Bc} = e^2 / \epsilon_c k_B T$ is the Bjerrum length at $\epsilon = \epsilon_c$. The second line of eq. (3.5) follows for the present choice $C = k_B T \chi / a^2$, where A and n_{iL} are defined by Eq.(2.11) and Eq.(2.18), respectively. Note that γ_p is independent of the ion density and increases with increasing the amphiphilic strength w_a from Eq.(2.17).

If $\gamma_p < 1$, $S(q)$ is maximum at $q = 0$ and we predict the usual phase transition in the mean field theory. In terms of the shift in Eq.(3.4) the spinodal $\chi = \chi_{\text{sp}}(\phi, n)$ is given by

$$\chi_{\text{sp}} = \frac{1}{2N_1 \phi} + \frac{1}{2N_2 (1 - \phi)} - \chi_c^{\text{ion}}. \quad (3.6)$$

The critical value of χ at given n , denoted by $\chi_c(n)$, is the minimum of χ_{sp} with respect to ϕ and is equal to χ_{sp} at $\phi = N_2^{1/2} / (N_1^{1/2} + N_2^{1/2})$. Thus,

$$\chi_c = \frac{1}{2N_1 N_2} (N_1^{1/2} + N_2^{1/2})^2 - \chi_c^{\text{ion}}. \quad (3.7)$$

For $N_1 = N_2 = 1$ we have $\chi_c = 2 - \chi_c^{\text{ion}}$. See Eqs.(5.1) and (5.2) and the right panel of Fig. 5 for the critical behavior below the transition ($\chi > \chi_c$). If we set $\bar{r} = a_0(T - T_c^0)$ at the critical composition, the critical temperature shift becomes $\Delta T_{\text{ion}} = \Delta r_{\text{ion}}/a_0$, where a_0 is a constant and T_c^0 is the critical temperature in the absence of ions. For the monovalent case we find $\Delta T_{\text{ion}} \sim k_B T_c (g_1 + g_2)^2 n / 4a_0$, where the factor $(g_1 + g_2)^2$ can be very large (~ 100). This result is consistent with previous experiments of binary mixtures with salt,^{26–28} where the coexistence curve has been observed to shift greatly with doping of small amounts of hydrophilic ions.

If $\gamma_p > 1$, the structure factor $S(q)$ attains a maximum at an intermediate wave number q_m given by

$$q_m = (\gamma_p - 1)^{1/2} \kappa. \quad (3.8)$$

The maximum of $S(q)$ is written as $S(q_m) = k_B T / (\bar{r} - r_m)$ with

$$r_m = \Delta r_{\text{ion}} + C_{\text{eff}} (\gamma_p - 1)^2 \kappa^2, \quad (3.9)$$

where we assume $\bar{r} > r_m$. For $\bar{r} < r_m$, a charge-density-wave phase should be realized. As long as $\gamma_p > 1$, this mesoscopic phase appears even for very small ion densities. For electrolytes, a mesoscopic phase was first predicted by Nabutovskii *et al.*,²⁹ who assumed the bilinear coupling $\rho\phi$ between the charge density ρ and the composition ϕ in the free energy. Recently, in their small-angle neutron scattering experiment, Sadakane *et al.*³⁰ found periodic structures in a binary mixture of D₂O-trimethylpyridine containing sodium tetrarphenylborate (NaBPh₄), where the scattered neutron intensity exhibited a peak at $q \sim 0.1/\text{\AA}$. Since this salt is composed of strongly hydrophilic and hydrophobic ions, we expect that the condition $\gamma_p > 1$ should have been satisfied. See the right panel of Fig. 5 for the ion distributions in such a case.

In polyelectrolytes, electric charges are attached to polymers and the structure factor of the polymer takes a form similar to that in Eq.(3.3), leading to a mesophase at low temperatures, in the Debye-Hückel approximation.^{31,32} In our theory, even a polymer solution consisting of neutral polymers and a polar solvent can exhibit a charge-density wave phase in the presence of a small amount of salt. This would explain a finding of a peak at an intermediate wave number in the scattering amplitude in polyethylene-oxide solutions with salt.³³

1.3.2. Effective interaction among charged particles

In a homogeneous phase with $\gamma_p < 1$, we may eliminate the composition fluctuations in F assuming their Gaussian distributions and setting $(\bar{r} + C_{\text{eff}}q^2)\phi_{\mathbf{q}} = k_B T \sum_i g_i n_i \mathbf{q}$. We then obtain attractive interactions among the ions mediated by the composition fluctuations. The resultant free energy of ions is written as

$$F_{\text{ion}} = \int d\mathbf{r} \sum_i k_B T n_i \ln(n_i a^3) + \frac{1}{2} \int d\mathbf{r} \int d\mathbf{r}' \sum_{i,j} V_{ij}(|\mathbf{r} - \mathbf{r}'|) \delta n_i(\mathbf{r}) \delta n_j(\mathbf{r}'), \quad (3.10)$$

where the deviations $\delta n_i = n_i - \langle n_i \rangle$ need not be small. The effective interaction potentials $V_{ij}(r)$ are expressed as

$$V_{ij}(r) = Q_i Q_j \frac{1}{\epsilon_c r} - \frac{(k_B T)^2}{4\pi C_{\text{eff}}} g_i g_j \frac{e^{-r/\xi}}{r}, \quad (3.11)$$

where $Q_1 = Z_1 e$ and $Q_2 = -Z_2 e$ are the ion charges and $\xi = (C_{\text{eff}}/\bar{r})^{1/2}$ is the correlation length. Among the ions of the same species ($i = j$), the second attractive term dominates over the first Coulomb repulsive term in the range $a \lesssim r \lesssim \xi$ when

$$g_i^2 > 4\pi C_{\text{eff}} Z_i^2 e^2 / \epsilon_c (k_B T)^2. \quad (3.12)$$

The right hand side is of order $4\pi Z_i^2 (1 - n_1/n_{1L}) \ell_{\text{Bc}}/a$ for low molecular-weight mixtures. Under the condition (3.12) there should be a tendency of aggregation of ions. This effect might explain a number of observations of micro-heterogeneities in near-critical binary mixtures containing salt.^{34,35}

It is also of great interest how charged colloid particles interact in polar solvent. There can be an attractive interaction among them in the presence of ion-composition or ion-polarization coupling. Such theory will be reported shortly.

1.4. Equilibrium conditions in one-dimensional cases and surface tension

We consider the equilibrium conditions around an interface in our system. The total free energy is the sum,

$$F = F_0 + F_{\text{sol}} + F_{\text{im}} + F_{\text{am}}. \quad (4.1)$$

We define the chemical potentials $\mu_i = \delta F / \delta n_i$ ($i = 1, 2, \dots$) of the ions and the chemical potential difference $h = \delta F / \delta \phi$ of the mixture. In equilibrium, these quantities are homogeneous constants.

1.4.1. Two species of ions

First we assume the presence of two species of ions. Some calculations yield

$$\mu_1 = k_B T [\ln c_1 + 1 + Z_1 U - g_1 \psi - \ln Z_{\text{am}}] + Z_1^2 \mu_{\text{im}}, \quad (4.2)$$

$$\mu_2 = k_B T [\ln c_2 + 1 - Z_2 U - g_2 \psi] + Z_2^2 \mu_{\text{im}}, \quad (4.3)$$

where $\psi = \phi - \phi_c$. If the first ion species has no amphiphilic character, we should set $Z_{\text{am}} = 1$. The μ_{im} is given by Eq.(2.10) in the 1D case. Here we equate the functional derivatives $\delta F_{\text{im}}/\delta n_i$ with $Z_i^2 \mu_{\text{im}}$ in Eq.(2.10) neglecting the ion-density dependence of κ . To get simpler expressions, we introduce normalized ion densities and potential by

$$c_1 = a^3 n_1, \quad c_2 = a^3 n_2, \quad U = e\Phi/k_B T. \quad (4.4)$$

Note that the ion sizes can be different from the size of the solvent molecules a . For example, the density of 10 mM salt is $n = 6 \times 10^{18} \text{cm}^{-3}$. If $a = 3\text{\AA}$, the normalized density $c = a^3 n$ is equal to 1.6×10^{-4} . The equilibrium ion densities are now expressed as

$$c_1 = c_{10} Z_{\text{am}} \exp[-Z_1 U + g_1 \psi - Z_1^2 \mu_{\text{im}}/k_B T], \quad (4.5)$$

$$c_2 = c_{20} \exp[Z_2 U + g_2 \psi - Z_2^2 \mu_{\text{im}}/k_B T], \quad (4.6)$$

where c_{10} and c_{20} are constants. Some calculations also give h in the form,

$$h = f'_0(\phi) - C \nabla^2 \phi - \frac{\varepsilon_1}{8\pi} \mathbf{E}^2 - k_B T (g_1 n_1 + g_2 n_2) + h_{\text{im}} + h_{\text{am}}, \quad (4.7)$$

where $f'_0 = \partial f_0/\partial \phi$ and the third term ($\propto \mathbf{E}^2$) is the functional derivative of the electrostatic energy with respect to ϕ .⁴ The $h_{\text{am}} = \delta F_{\text{am}}/\delta \phi$ is the contribution from the amphiphilic interaction. In the 1D case, h_{im} is given by the right hand side of Eq.(2.10) with $d\psi(z')/dz'$ being replaced by $\sum_i Z_i^2 dn_i(z')/dz'$, while h_{am} is expressed as

$$\frac{h_{\text{am}}(z)}{k_B T} = \frac{w_a}{2\ell} \int_{-\ell}^{\ell} d\zeta X(z + \zeta) \left[e^{w_a[\phi(z+2\zeta) - \phi(z)]} - e^{w_a[\phi(z) - \phi(z+2\zeta)]} \right]. \quad (4.8)$$

Here we define $X(z) = n_1(z)/Z_{\text{am}}(z)$.

In the 1D case, the charge neutrality should be satisfied as $z \rightarrow \pm\infty$. If $\phi \rightarrow \phi_\alpha$ as $z \rightarrow -\infty$ and $\phi \rightarrow \phi_\beta$ as $z \rightarrow \infty$, Eqs.(4.2) and (4.3) yield the general relations (1.3) and (1.4). Under Eq.(2.6) they are rewritten as

$$e(\Phi_\alpha - \Phi_\beta) = k_B T \frac{g_1 - g_2}{Z_1 + Z_2} \Delta\phi, \quad (4.9)$$

$$\frac{n_{1\beta}}{n_{1\alpha}} = \frac{n_{2\beta}}{n_{2\alpha}} = \exp \left[- \frac{Z_2 g_1 + Z_1 g_2}{Z_1 + Z_2} \Delta\phi \right], \quad (4.10)$$

where $\Delta\phi = \phi_\alpha - \phi_\beta$. The image and amphiphilic interactions vanish far from the interface and do not affect the above relations.

1.4.2. Three species of ions

Performing x-ray reflectivity measurements, Luo *et al.*³⁶ measured the ion distributions in the vicinity of an interface in water-nitrobenzene. They added two salts, tetrabutylammonium tetraphenylborate (TBA-TPB) and tetrabutylammonium bromide (TBA-Br). Then they realized a two-phase state with hydrophilic anion Br^- , hydrophobic cation TBA^+ , and hydrophobic anion TPB^- . They detected strong accumulation or depletion of the ions on the two sides of the interface, which suggest a crucial role of the ion-solvent interactions dependent on the ion and solvent species. In our scheme, numerical analysis is needed to calculate such complicated ion distributions, as will be exemplified in Fig. 6 below.

Here we examine how the potential difference $\Delta\Phi$ in Eq.(1.3) is related to the bulk ion densities for three ion species.⁶ Let them have charges, $Q_1 = eZ_1$, $Q_2 = -eZ_2$, and $Q_3 = -eZ_3$. If the anions 2 and 3 have no amphiphilic character, the normalized density of the third species $c_3 = a^3 n_3$ is given in the form of Eq.(4.6) if the subscript 2 is replaced by 3. Again, α and β denote the more polar (water-rich) phase and the less polar (water-poor) phase, respectively. To avoid cumbersome notation, we define the normalized chemical potential differences $\nu_i = \Delta\mu_{\alpha\beta}^i/k_B T$ ($i = 1, 2, 3$) and normalized potential difference $\Delta U = e(\Phi_\alpha - \Phi_\beta)/k_B T$. Then,

$$\frac{c_{1\beta}}{c_{1\alpha}} = e^{Z_1 \Delta U - \nu_1}, \quad \frac{c_{2\beta}}{c_{2\alpha}} = e^{-Z_2 \Delta U - \nu_2}, \quad \frac{c_{3\beta}}{c_{3\alpha}} = e^{-Z_3 \Delta U - \nu_3}, \quad (4.11)$$

where $\nu_i = g_i \Delta\phi$ with $\Delta\phi = \phi_\alpha - \phi_\beta$. The charge neutrality conditions are $Z_1 c_{1\alpha} = Z_2 c_{2\alpha} + Z_3 c_{3\alpha}$ and $Z_1 c_{1\beta} = Z_2 c_{2\beta} + Z_3 c_{3\beta}$ in the bulk two phases. In terms of the ion densities in the α phase, it follows the equation for ΔU in the form,

$$(Z_2 c_{2\alpha} + Z_3 c_{3\alpha}) e^{Z_1 \Delta U - \nu_1} = Z_2 c_{2\alpha} e^{-Z_2 \Delta U - \nu_2} + Z_3 c_{3\alpha} e^{-Z_3 \Delta U - \nu_3}. \quad (4.12)$$

In the monovalent case $Z_1 = Z_2 = Z_3 = 1$, the above equation is simplified to

$$e^{2\Delta U} = (c_{2\alpha} e^{\nu_1 - \nu_2} + c_{3\alpha} e^{\nu_1 - \nu_3}) / (c_{2\alpha} + c_{3\alpha}), \quad (4.13)$$

which reduces to the expression (1.3) (independent of $c_{2\alpha}$) for $c_{3\alpha} = 0$.

However, in the experiment,³⁶ the third species (TPB^-) was strongly hydrophobic such that $c_{3\alpha} \ll c_{3\beta}$ was realized, while the second species

(Br⁻) was hydrophilic. Supposing such cases, let us assume $g_2 > 0$ and $g_3 < 0$ and choose $c_{2\alpha}$ and $c_{3\beta}$ as control parameters. If we set

$$X = \exp[\Delta U - (\nu_1 - \nu_2)/2], \quad (4.14)$$

Eq.(4.1) becomes a cubic equation,

$$X - X^{-1} = 2R[1 - X^2 e^{\nu_3 - \nu_2}]. \quad (4.15)$$

where we define

$$R = e^{(\nu_1 + \nu_2)/2} c_{3\beta} / 2c_{2\alpha}. \quad (4.16)$$

We may well assume $X^2 e^{\nu_3 - \nu_2} \ll 1$ for large $|g_3| \gg 1$ to obtain $X \cong R + \sqrt{1 + R^2}$ or

$$\frac{e}{T} \Delta \Phi \cong \frac{1}{2}(\nu_1 - \nu_2) + \ln(R + \sqrt{1 + R^2}), \quad (4.17)$$

If $\nu_1 + \nu_2 \gg 1$, we readily reach the regime $R \gg 1$ even at small $c_{3\beta}$, where $X \cong 2R$ and $X^2 e^{\nu_3 - \nu_2} \cong (c_{3\beta}/c_{2\alpha})^2 e^{\nu_1 + \nu_3}$. That is, we find

$$\Delta U \cong \nu_1 + \ln(c_{3\beta}/c_{2\alpha}), \quad (4.18)$$

for $e^{-(\nu_1 + \nu_2)/2} \ll c_{3\beta}/c_{2\alpha} \ll e^{-(\nu_1 + \nu_3)/2}$. In this case, $c_{1\alpha} \cong c_{2\alpha}$, $c_{1\beta} \cong c_{3\beta}$, $c_{2\beta} \cong e^{-(\nu_1 + \nu_2)} c_{2\alpha}^2 / c_{3\beta} \ll c_{3\beta}$, and $c_{3\alpha} \cong e^{\nu_1 + \nu_3} c_{3\beta}^2 / c_{2\alpha} \ll c_{2\alpha}$.

1.4.3. Surface tension

As stated in Section 1, the surface tension γ of a water-air interface has been observed to increase with increasing the amount of small hydrophilic ions in water. However, for a pair of hydrophilic and hydrophobic ions, it can decrease with increasing the salt density even without amphiphilic interaction (see the right panel of Fig. 5).⁴ It is well-known that the surfactant molecules accumulate at the interface and γ decreases with increasing the surfactant density.¹⁸ We here examine the behavior of γ for the case $\gamma_p < 1$, where γ_p is the asymmetry parameter defined by Eq.(3.5).

To calculate γ we introduce the grand potential by

$$\Omega = \int d\mathbf{r} \omega = F - \int d\mathbf{r} (h\phi + \sum_i \mu_i n_i). \quad (4.19)$$

For given constant h , μ_1 , μ_2 , \dots , Ω is minimized as a functional of ϕ , n_1 , n_2 , \dots in equilibrium, yielding Eqs.(4.2), (4.3), and (4.7). In our system the grand potential density ω is expressed as

$$\omega = f_0(\phi) + \frac{C}{2} |\nabla \phi|^2 - h\phi - k_B T n - \rho \Phi + \frac{\varepsilon}{8\pi} \mathbf{E}^2, \quad (4.20)$$

where $n = \sum_i n_i$. Use has been made of Eqs.(4.2) and (4.3) to eliminate μ_i . We suppose a planar interface perpendicular to the z axis; then, $\omega(z)$ should tend to a common constant ω_∞ as $z \rightarrow \pm\infty$. To show this, we calculate the space derivative,

$$\frac{d}{dz} \left[\omega - C(\psi')^2 + \rho\Phi \right] = \sum_i n_i Z_i^2 \frac{d\mu_{im}}{dz} + n_1 \frac{d\mu_{am}}{dz} - (h_{im} + h_{am})\psi', \quad (4.21)$$

where $\psi' = d\psi/dz$ and $\mu_{am} = -k_B T \ln Z_{am}$ (see Eq.(2.19)). The h_{im} and h_{am} are defined by Eqs.(4.7) and (4.8). Note that F_{im} and F_{am} are invariant with respect to a small displacement $\delta\zeta$ of the interface position or with respect to the change of ψ and n_i to $\psi - \psi'\delta\zeta$ and $n_i - n'_i\delta\zeta$, respectively, where $n'_i = dn_i/dz$. Then we find

$$\int dz [h_{im}\psi' + \sum_i \mu_{im}^i n'_i] = 0, \quad \int dz [h_{am}\psi' + \mu_{am} n'_1] = 0, \quad (4.22)$$

where we have pushed the lower and upper bounds of the integrals to $\mp\infty$. Owing to these relations, the z integration of the right hand side of Eq.(4.21) vanishes, leading to $\omega(z) \rightarrow \omega_\infty$ as $z \rightarrow \pm\infty$. It is convenient to express the surface tension $\gamma = \int dz [\omega(z) - \omega_\infty]$ as

$$\gamma = \int dz \left[f_0(\phi) + \frac{C}{2} |\nabla\phi|^2 - k_B T n - h\phi - C_\alpha \right] - \int dz \frac{\varepsilon(\phi)}{8\pi} E^2, \quad (4.23)$$

where $C_\alpha = f_0(\phi_\alpha) - k_B T n_\alpha - h\phi_\alpha$ and

$$h = [f_0(\phi_\alpha) - f_0(\phi_\beta) - k_B T (n_\alpha - n_\beta)] / \Delta\phi \quad (4.24)$$

with n_α and n_β being the bulk values of n and the integrand of the first term vanishes as $z \rightarrow \pm\infty$. From Eq.(2.4) the electric field is expressed as $E(z) = -\Phi'(z) = 4\pi\varepsilon(z)^{-1} \int_{-\infty}^z dz' \rho(z')$. There should be no net charge or $\int_{-\infty}^{\infty} dz \rho(z) = 0$ around the interface if $E(z) \rightarrow 0$ far from the interface.

Away from the ion-induced critical point, we are interested in the excess surface tension $\Delta\gamma = \gamma - \gamma_0$, where γ_0 is the surface tension without ions. Let $\phi(z) \rightarrow \phi_0(z)$ and $h \rightarrow h_0$ as $n \rightarrow 0$. We expand $\omega(z)$ in Eq.(4.20) with respect to the deviation $\delta\phi = \phi - \phi_0$. Neglecting the terms of order $(\delta\phi)^2$, we obtain $h - h_0 \cong -k_B T (n_\alpha - n_\beta) / \Delta\phi$ and⁴

$$\Delta\gamma \cong -k_B T \Gamma - \int dz \frac{\varepsilon(\phi)}{8\pi} E^2, \quad (4.25)$$

where Γ is the adsorbed ion density defined by

$$\Gamma = \int_{-\infty}^{z_{\text{int}}} dz [n(z) - n_\alpha] + \int_{z_{\text{int}}}^{\infty} dz [n(z) - n_\beta]. \quad (4.26)$$

The interface position z_{int} is determined by the Gibbs construction,²⁵

$$\phi_{\alpha} z_{\text{int}} + \phi_{\beta}(L - z_{\text{int}}) = \int_0^L dz \phi(z), \quad (4.27)$$

in a finite system in the region $0 < z < L$ with $L \gg \xi$. In Eq.(4.25) the lower and upper bounds far from the interface are pushed to infinity. If the last term in Eq.(4.25) is neglected, we obtain the Gibbs equation $\Delta\gamma = -k_B T \Gamma$ at relatively low adsorption.²⁵ The adsorbed density Γ can be much enhanced for surfactants, while it is negative for low-density hydrophilic ions at an water-air interface.

The last negative term in Eq.(4.23) or Eq.(4.25) arises from the last two terms in Eq.(4.20), which is written as γ_e . In all the examples in our previous work,⁴ it was at most a few percents of $\Delta\gamma$. To roughly estimate it, let us employ the Poisson-Boltzmann equation $dU(z)^2/dz^2 = \kappa_{\beta}^2 \sinh(U(z) - U_{\beta})$ in the region $z > z_{\text{int}}$ and $dU(z)^2/dz^2 = \kappa_{\alpha}^2 \sinh(U(z) - U_{\alpha})$ in the region $z < z_{\text{int}}$, where κ_{α} and κ_{β} are the Debye-Hückel wavenumber. Here we take the thin interface limit $\xi \rightarrow 0$ and neglect the image potential. We impose the continuity of U and $\varepsilon dU/dz$ at the interface. Then γ_e is approximated by the Poisson-Boltzmann result,

$$\gamma_e^{\text{PB}} = -2k_B T \frac{n_{\alpha}}{\kappa_{\alpha}} \left[\sqrt{1 + b^2 + 2b \cosh(\Delta U/2)} - 1 - b \right], \quad (4.28)$$

where $b = \varepsilon_{\beta} \kappa_{\beta} / \varepsilon_{\alpha} \kappa_{\alpha} = (\varepsilon_{\beta} n_{\beta} / \varepsilon_{\alpha} n_{\alpha})^{1/2}$, with ε_{α} and ε_{β} being the dielectric constants in the bulk phases, and $\Delta U = U_{\alpha} - U_{\beta} = (g_1 - g_2) \Delta\phi/2$ is the normalized potential difference. Here $\gamma_e^{\text{PB}} = 0$ for $g_1 = g_2$, so we assume $(g_1 - g_2) \Delta\phi > 1$. Typical behaviors of γ_e^{PB} in the monovalent case are as follows. (i) If g_1 and g_2 are both considerably larger than unity with $g_1 > g_2$, we have $b \sim e^{-(g_1 + g_2) \Delta\phi/4} \ll 1$ and $b e^{\Delta U/2} = e^{-g_2 \Delta\phi/2} \ll 1$, so that $a^2 |\gamma_e^{\text{PB}}| / k_B T \sim a \kappa_{\alpha} e^{-g_2 \Delta\phi/2} / A \ll 1$, where A is defined by Eq.(2.11). This result is consistent with our previous results.⁴ (ii) In the case $g_1 = -g_2 \gg 1$, we have $\Delta U = g_1 \Delta\phi$ and $b \sim 1$. Then $a^2 |\gamma_e^{\text{PB}}| / k_B T \sim a \kappa_{\alpha} e^{g_1 \Delta\phi/4} / A$ grows with increasing g_1 . This case will be numerically examined in the right panel of Fig. 2.

Note the relation $\gamma_e^{\text{PB}} \propto n_{\alpha}^{1/2}$, leading to the square root dependence of $\Delta\gamma$ at low ion densities. In Fig. 5, we shall see this dependence for hydrophilic and hydrophobic ion pairs. On the other hand, for hydrophilic pairs, we propose the following form,

$$\Delta\gamma/T \cong -A_s (n_{\alpha} / \ell_{B\alpha})^{1/2} + \lambda_s n_{\alpha}, \quad (4.29)$$

where $\ell_{B\alpha}$ is the Bjerrum length in the α phase, The coefficient A_s is small, while the second term is of the well-known form accounting for the ion depletion. With this form, $\Delta\gamma$ should exhibit a small minimum given by

$$(\Delta\gamma)_{\min} = -T\lambda_s n_m \tag{4.30}$$

at $n = n_m = (A_s/2\lambda_s)^2/\ell_{B\alpha}$. As an example, let the ion concentration giving this minimum be 1 mM in the water-rich phase. Then we obtain $A_s = 1.2 \times 10^{-2}$ by setting $\lambda_s = 3\text{\AA}$ and $\ell_{B\alpha} = 7\text{\AA}$.

For water-air interfaces, Jones and Ray¹³ found a negative minimum in $\Delta\gamma$ of order $-10^{-4}\gamma_0$. We notice that their data can well be fitted to Eq.(4.29) with $A_s \sim 10^{-2}$. However, we have assumed appreciable ion densities even in the less polar β region. That is, our one-dimensional calculations are justified only when the screening length κ_β^{-1} in the β region is much shorter than any characteristic lengths in experiments, which are the inverse curvature of the meniscus or the wavelength of capillary waves, for example. In the literature^{10-12,16} ions are treated to be nonexistent in the air region, so we do not still understand the Jones-Ray effect.

1.5. Numerical results of ion distributions

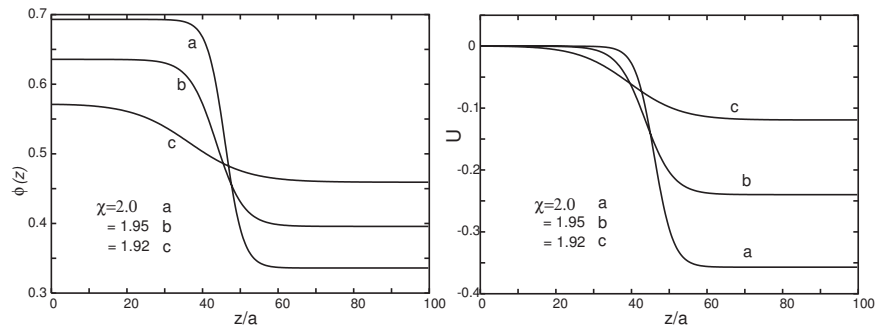


Fig. 1.1. Composition $\phi(z)$ (left) and normalized electric potential $U(z)$ (right) on approaching the criticality as $\chi = 2, 1.95,$ and 1.92 with $c_{1\alpha}c_{1\beta} = 10^{-4}$. The ions are both hydrophilic with $g_1 = 4$ and $g_2 = 2$. The critical value of χ is 1.91 from Eq.(3.7).

In the one-dimensional geometry, we display equilibrium profiles of the composition and the ion densities and calculate the surface tension for various parameter values. In the monovalent case, we set $A = 4$ (except in the left panel of Fig.4) and $\epsilon_1/\epsilon_c = 0.8$. The dielectric constant of the α phase is twice larger than that of the β phase at $\chi = 3$, so the inhomogeneity

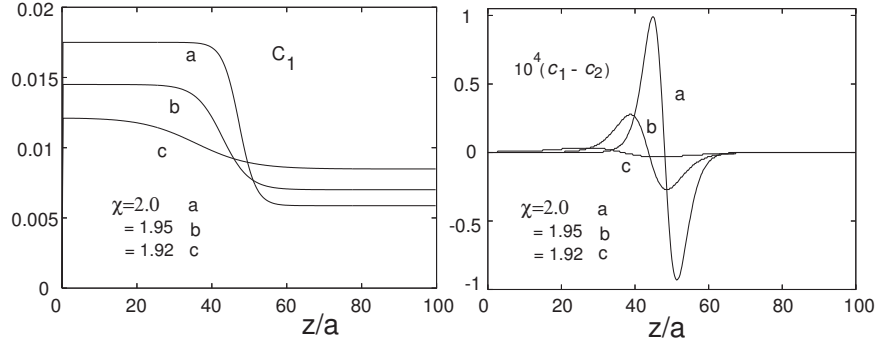


Fig. 1.2. Normalized ion density $c_1(z)$ (left) and normalized charge density $c_1(z) - c_2(z)$ (multiplied by 10^4) (right) with varying χ with the same parameter values as in Fig. 1.

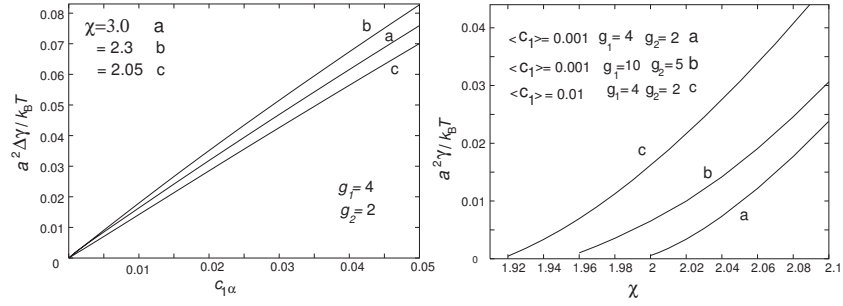


Fig. 1.3. Left: Normalized excess surface tension $a^2\Delta\gamma/k_B T$ versus $c_{1\alpha}$, obeying Eq.(1.6). Right: Normalized surface tension $a^2\gamma/k_B T$ as a function of χ . It tends to zero as $\chi \rightarrow \chi_c$. The two ion species are both hydrophilic in these cases.

of the dielectric constant is rather mild. The condition $\gamma_p < 1$ is satisfied in all the examples (see the discussion around Eq.(3.5)). In the following figures, we give profiles along the z axis, where the α phase is on the left and the β phase is on the right.

1.5.1. Including solvation and image interactions

We first assume no amphiphilic interaction. In Fig. 1, we show the composition $\phi(z)$ and the normalized electric potential $U(z) = e\Phi(z)/k_B T$ (taken to be zero in the α phase) near an interface for three values of χ with $g_1 = 4$ and $g_2 = 2$, where we fix the product $c_{1\alpha}c_{1\beta} = 10^{-4}$. As χ is decreased with $\gamma_p < 1$, we approach the critical point dependent on the salt den-

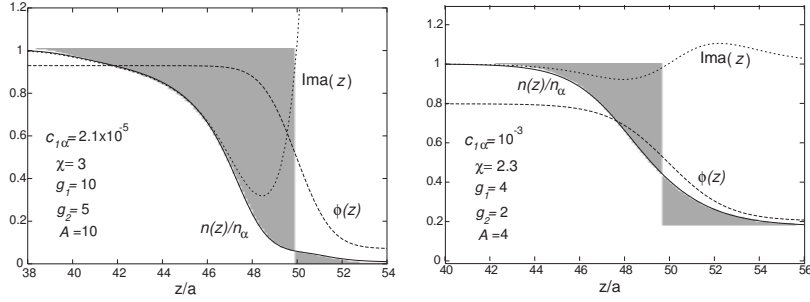


Fig. 1.4. Normalized ion density $n(z)/n_\alpha$, composition $\phi(z)$, and image factor $I_{\text{ma}}(z)$ for $\chi = 3$, $g_1 = 10$, $g_2 = 5$, and $c_{1\alpha} = 2.1 \times 10^{-5}$ (left) and for $\chi = 2.3$, $g_1 = 4$, $g_2 = 2$, and $c_{1\alpha} = 10^{-3}$ (right). The gray regions correspond to the two terms in Γ in Eq.(4.26). From the curves of $I_{\text{ma}}(z)$, the image interaction serves to repel the ions from the interface on the left, while it is not important on the right.

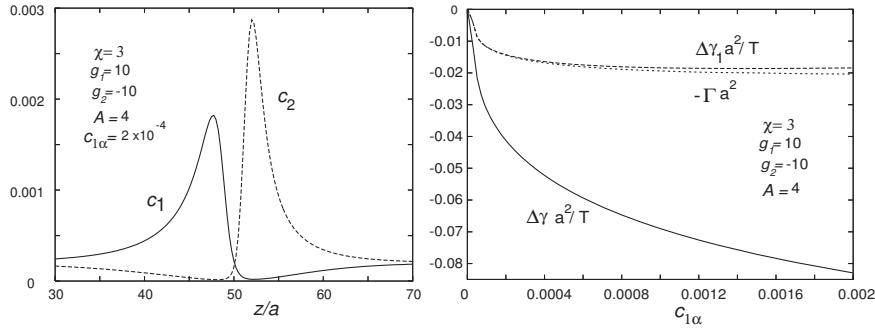


Fig. 1.5. Left: Normalized ion densities, where $\chi = 3$, $A = 4$, $g_1 = -g_2 = 10$, and $c_{1\alpha} = c_{1\beta} = 2 \times 10^{-4}$. For this hydrophilic and hydrophobic ion pair, a microphase separation forming a large electric double layer is apparent. Right: $a^2\Delta\gamma/T$ and $a^2\Delta\gamma_1/T$ as functions of $c_{1\alpha}$, where γ_1 is the first term in Eq.(2.23) and $\Delta\gamma_1 = \gamma_1 - \gamma_0$ is very close to $-\Gamma a^2$. This shows that the electrostatic part $\gamma_e = \gamma - \gamma_1 = -\int dz \varepsilon E^2/8\pi$ dominates over $\Delta\gamma_1 \cong -k_B T T$.

sity, as discussed in Section 3. The critical value of χ is given by Eq.(3.7). The electric potential jump is given by Eq.(4.9). In Fig. 2, we display the ion density $c_1(z)$ and the normalized charge density $c_1(z) - c_2(z)$. The ion densities are reduced in the β phase as in Eq.(4.10). We can see that an electric double layer at the interface diminishes as the critical point is approached. It is convenient to choose $\bar{n} \equiv (n_\alpha n_\beta)^{1/2} (= 2(c_{1\alpha} c_{1\beta})^{1/2}/a^3$ in the monovalent case) in two phase states as the parameter representing the degree of ion doping.⁴ Over a rather wide parameter region, the bulk

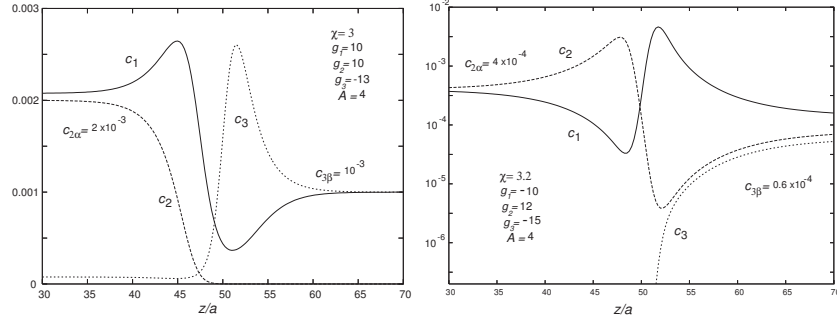


Fig. 1.6. Left: Normalized ion densities $c_1(z)$, $c_2(z)$, and $c_3(z)$ in the presence of three ion species with $g_1 = g_2 = 10$ and $g_3 = -13$. The second species does not penetrate into the β region. Right: Those for $g_1 = -10$, $g_2 = 12$, and $g_3 = -13$ on a semi-logarithmic scale, resembling to those in the experiment.³⁶ The third species does not penetrate into the α region.

concentrations in the two phases are expressed as

$$\frac{1}{2}(\phi_\alpha + \phi_\beta) - \frac{1}{2} \cong \frac{1}{32} [(g_1 Z_2 + g_2 Z_1)/(Z_1 + Z_2)]^3 a^3 \bar{n}, \quad (5.1)$$

$$\Delta\phi = \phi_\alpha - \phi_\beta \cong [3(\chi - \chi_c)/2]^{1/2}, \quad (5.2)$$

where use has been made of the Landau expansion of the free energy density f_0 in Eq.(2.3). The first line is the shift of the critical composition. The second line is the usual mean field expression for the average order parameter difference. These relations are consistent with Figs. 1 and 2.

The surface tension γ can be calculated numerically from Eq.(4.23) using Eq.(4.24). In Fig.3, we show the excess surface tension $\Delta\gamma = \gamma - \gamma_0$ versus $c_{1\alpha}$ when the two ion species are both hydrophilic, in accord with the experiments.¹³⁻¹⁵ Without ions, we find $a^2\gamma_0/k_B T = 0.498$, 0.103 , and 0.0773 for $\chi = 3$, 2.3 , and 2.05 , respectively. Though these γ_0 values are very different, $\Delta\gamma$ increases roughly linearly with increasing the ion density. The right panel of Fig. 3 displays the surface tension γ itself for three cases, where the interface is located at the middle of the cell and the space average $\langle c_1 \rangle$ is fixed. For each curve the critical value χ_c is given by Eq.(3.7) and γ tends to zero as $\chi \rightarrow \chi_c$.

We illustrate how the two terms in Eq.(4.26) can be interpreted graphically, where the two ion species are both hydrophilic and the electrostatic term, the third term in Eq.(4.25), is negligible. We also demonstrate relevance of the image interaction at small ion densities. In Fig. 4, we display

the normalized ion density $n(z)/n_\alpha$, the composition $\phi(z)$, and the image factor defined by

$$\text{Ima}(z) = \exp[-\mu_{\text{im}}(z)/k_B T], \quad (5.3)$$

in the monovalent case. This factor appears in c_1 and c_2 in Eqs.(4.5) and (4.6). In Fig. 4, the areas of the left and right gray regions multiplied by $n_\alpha a$ are equal to the first term and the minus of the second term in Eq.(4.26), respectively. The ion density $n(z)$ is shifted to the left of the interface at $z = z_{\text{int}} (\cong 50a)$. This means that the ions are repelled from the interface in the α phase. We furthermore mention detailed characteristic features. (i) In the left panel, we set $\chi = 3$, $c_{1\alpha} = 2.1 \times 10^{-5}$, $g_1 = 10$, $g_2 = 5$, and $A = 10$, where the ion density is very small and $1/2\kappa_\alpha = 6.7a$ is rather long. The first term of Eq.(4.26) is 103.5% of the total $a^2 \Delta\gamma/k_B T = 7.32c_{1\alpha}$. The formula (1.6) can be used in this example. See the discussion around Eq.(2.12). (ii) In the right panel, we set $\chi = 2.3$, $c_{1\alpha} = 10^{-3}$, $g_1 = 4$, $g_2 = 2$, and $A = 4$, where the ion density is relatively large and the ion reduction factor in Eq.(4.10) ($\sim e^{-1.8}$) is not very small. The first term in Eq.(4.26) is then 158% of the total $\Delta\gamma/k_B T = 2.03a^{-2}c_{1\alpha}$. In this case $\text{Ima}(z) \cong 1$ at any z , so the image interaction is not important.

The ion distributions for a pair of strongly hydrophilic and hydrophobic ions are very singular. In the left panel of Fig. 5, we show $c_1(z)$ and $c_2(z)$ for with $g_1 = -g_2 = 10$ at $\chi = 3$, where Eq.(3.5) gives $\gamma_p = 5/4\sqrt{3} < 1$. Notice that $c_{1\alpha}$ and $c_{1\beta}$ coincide from Eq.(4.10) and is set equal to 2×10^{-4} . Here $\Delta\gamma = -0.041Ta^{-2}$ and $\Gamma = 0.014a^{-2}$. We can see a marked growth of the electric double layer and a deep minimum in the ion density $c_1 + c_2$ at the interface position. In our previous work,⁴ we obtained milder ion profiles for $g_1 = -g_2 = 4$. In the right panel of Fig. 5, we examine how $\Delta\gamma = \gamma - \gamma_0$ and $\Delta\gamma_1 = \gamma_1 - \gamma_0$ are decreased with increasing $c_{1\alpha}$ for $g_1 = -g_2 = 10$, where γ_1 is the first term on the right hand side of Eq.(4.23). We notice the following. (i) The changes $\Delta\gamma$ and $\Delta\gamma_1$ are both proportional to $c_{1\alpha}^{1/2}$ at small $c_{1\alpha}$. Here $|\Delta\gamma|/c_{1\alpha}^{1/2}$ is of order unity, so $\Delta\gamma$ is appreciable even for very small $c_{1\alpha}$. (ii) The electrostatic part $\gamma_e = -\int dz \varepsilon E^2/8\pi$ is known to be important in this case from comparison between $\Delta\gamma_1$ and $\Delta\gamma = \Delta\gamma_1 + \gamma_e$. (iii) We confirm that the modified Gibbs relation $\Delta\gamma_1 \cong -k_B T \Gamma$ holds excellently.

In Fig. 6, we display the ion distributions in the presence of three ion species in the monovalent case with $Q_1 = e$, $Q_2 = -e$, and $Q_3 = -e$. Since the absolute values of g_i are taken to be large, we can see steep and complex variations of the ion distributions around the interface. In

the left panel, the first and second species are both hydrophilic but the third one is hydrophobic as $g_1 = g_2 = 10$ and $g_3 = -13$, where $\chi = 3$, $e(\Phi_\alpha - \Phi_\beta)/T = 7.92$, and $\gamma = 0.446T/a^2$. This is the case discussed around Eqs.(4.17) and (4.18), since $X^2 e^{(g_3 - g_2)\Delta\phi} = 1.5 \times 10^{-2}$ and $R = 2.7 \times 10^3$. In the right panel, the first and third species are hydrophobic but the second species is hydrophilic as $g_1 = -10$, $g_2 = 12$, and $g_3 = -15$, where $\chi = 3.2$, $e(\Phi_\alpha - \Phi_\beta)/T = 7.01$, and $\gamma = 0.600T/a^2$ (with $\gamma_0 = 0.620T/a^2$). The ion distributions in this latter case can be compared with those in the experiment by Luo *et al.*,³⁶ so the curves are written on a semilogarithmic scale as in their paper. The adopted parameter values are inferred from their experimental data.

1.5.2. Including amphiphilic interaction in addition to solvation and image interactions

We give numerical results including the amphiphilic interaction in addition to the solvation and image interactions. We set $2\ell = 5a$ and change w_a . In Fig. 7, we show c_1 , c_2 , and U with $w_a = 12$ for two ion densities, $c_{1\alpha} = 10^{-3}$ and 2×10^{-3} . The other parameter values are $\chi = 3$, $g_1 = 4$, and $g_2 = 8$, so the counterions are more strongly repelled from the interface into the α phase. We can see marked adsorption of the ions at the interface. For $n_{i\alpha} \geq n_{i\beta}$ we define the areal densities of adsorbed ions by

$$\Gamma_i^> = \int_{n_i > A_{\text{th}} n_{1\alpha}} dz [n_i(z) - n_{i\alpha}] \quad (i = 1, 2), \quad (5.4)$$

where the integration is in the region with $n_i(z) > A_{\text{th}} n_{1\alpha}$. We set $A_{\text{th}} = 1.05$ here. In Fig. 7, $(a^2\Gamma_1^>, a^2\Gamma_2^>)$ is given by $(0.034, 0.029)$ for $c_{1\alpha} = 10^{-3}$ and by $(0.091, 0.085)$ for $c_{1\alpha} = 2 \times 10^{-3}$. We have $\gamma = 0.497$, 0.426 , and 0.336 for $c_{1\alpha} = 0$, 10^{-3} , and 2×10^{-3} , respectively, in units of $k_B T/a^2$. The distribution of the counterions is wider than that of the ionic surfactant. The normalized potential $U(z)$ has a peak at $z = z_p$ near the interface and slowly relaxes in the β phase on the scale of the screening length κ_β^{-1} .

In Fig. 8, we examine the case of hydrophilic cations and hydrophobic anions with $g_1 = -g_2 = 8$ for the two cases of $w_a = 0$ and 8 by setting $c_{1\alpha} = 10^{-3}$ and $\chi = 3$. The adsorbed densities defined by Eq.(5.4) are $(a^2\Gamma_1^>, a^2\Gamma_2^>) = (0.043, 0.040)$ for $w_a = 8$. The surface tension is 0.497 and 0.402 for $w_a = 0$ and 8 , respectively, in units of $k_B T/a^2$. In this case, the electric double layer is enlarged and ΔU is a monotonically decreasing function of z .

In Fig. 9, we examine how the surface tension γ decreases to zero and how the adsorption increases with increasing w_a (left) and $c_{1\alpha}$ (right) in our 1D calculations. In the left panel, the accumulation occurs rather abruptly for $w_a \gtrsim 5$, where $g_1 = -g_2 = 8$, $\chi = 3$, and $c_{1\alpha} = 10^{-3}$. This behavior is consistent with Eq.(2.21). In the right panel, where $g_1 = 4$, $g_2 = 2$, $\chi = 3$, and $w_a = 12$, the adsorbed densities $\Gamma_1^>$ and $\Gamma_2^>$ increase linearly as $87c_{1\alpha}a^{-2}$ and $64c_{1\alpha}a^{-2}$, respectively, and the surface tension decreases as $\gamma = (0.497 - 177c_{1\alpha})k_B T/a^2$ at small $c_{1\alpha}$. We notice the following. (i) We find $\Gamma (\cong \Gamma_1^> + \Gamma_2^>)$ is proportional to $n_\alpha = 2v_0^{-1}c_{1\alpha}$. In the literature, the Langmuir adsorption isotherm $\Gamma = \Gamma_{\max}Kn/(1 + Kn)$ is well-known, where n is the surfactant density far from the interface with Γ_{\max} and K being constants. It predicts $\Gamma \propto n$ for $n \ll K^{-1}$. (ii) Our results are roughly in accord with the Gibbs adsorption equation $\Delta\gamma = -k_B T\Gamma$ at low surfactant densities, where a rather small discrepancy arises from the third electrostatic term in Eq.(4.25) in the present case.

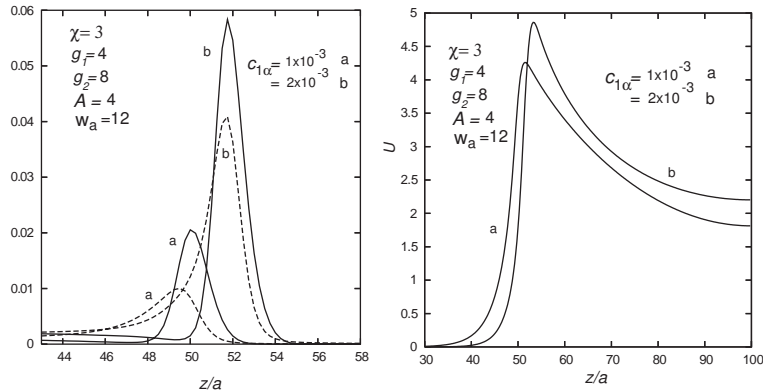


Fig. 1.7. Normalized cationic-surfactant density c_1 (bold line) and counterion density c_2 (broken line) in the left panel, and normalized electric potential U in the right panel, where (a) $c_{1\alpha} = 10^{-3}$ and (b) 2×10^{-3} with $g_1 = 4$ and $g_2 = 8$. The excess surfactant density accumulated on the interface is $\Gamma_1^> = 0.034a^{-2}$ in (a) and $0.091a^{-2}$ in (b).

1.6. Summary and remarks

We summarize our results.

(i) We have introduced the composition-dependent solvation chemical potentials in Eq.(2.3). The solvation chemical potential μ_{sol} in Eq.(2.6) is bilinear with respect to ϕ and c_i and is characterized by the parameters

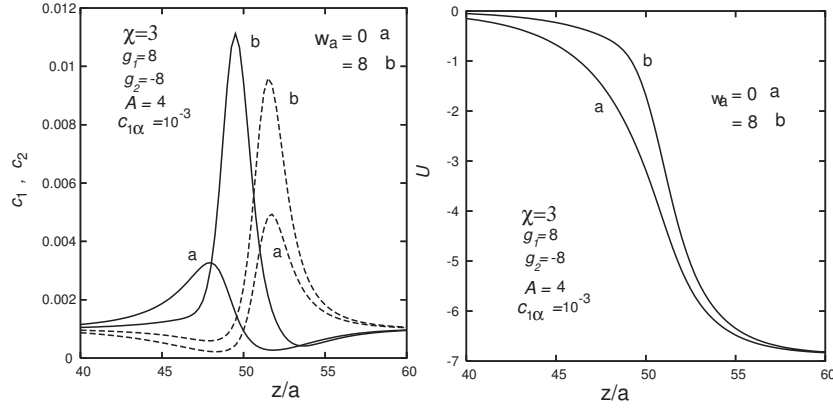


Fig. 1.8. Normalized cation density c_1 (bold line) and anion density c_2 (broken line) in the left panel and normalized electric potential U in the right panel, where $g_1 = -g_2 = 8$, and $c_{1\alpha} = 10^{-3}$. Here (a) $w_a = 0$ (no amphiphilic interaction) and (b) $w_a = 8$ (surfactant). The excess cation density accumulated on the interface is $\Gamma_1^> = 0.005a^{-2}$ in (a) and $0.040a^{-2}$ in (b). The surface tension decreases with increasing w_a as in the right panel of Fig. 9.

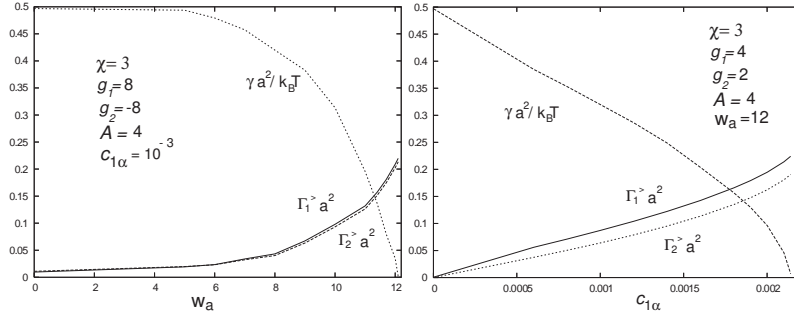


Fig. 1.9. Normalized surface tension $a^2\gamma/k_B T$, normalized adsorbed cationic-surfactant and counterion densities $a^2\Gamma_1^>$ and $a^2\Gamma_2^>$ as functions of w_a (left) and of $c_{1\alpha}$ (right). Here $g_1 = -g_2 = 8$, and $c_{1\alpha} = 10^{-3}$ (left). and $g_1 = 4, g_2 = 2$, and $w_a = 12$ (right).

g_i dependent on the ion species i . For aqueous mixtures, $g_i > 0$ for hydrophilic ions, while $g_i < 0$ for hydrophobic ions. In the asymmetric case $g_1 \neq g_2$, the Galvani potential difference arises at an interface.

(ii) The image chemical potential stems from the composition-dependence of the dielectric constant $\epsilon(\phi)$ in Eq.(2.5), as expressed in the integral form (2.6). It can be important around an interface where ϵ changes abruptly. For a pair of strongly hydrophilic cations and anions, the ions are signifi-

cantly repelled from the interface when the screening length κ_α^{-1} is longer than the Bjerrum length $\ell_{B\alpha}$ in the strongly segregated case.

(iii) When hydrophilic and hydrophobic ions coexist, there appears a tendency of microphase separation at an interface, as is evident in Fig. 5. The surface tension decreases drastically for large $|g_1|$ and $|g_2|$ (even without amphiphilic interaction), where the electrostatic contribution to the surface tension, the last term in Eq.(4.23) or Eq.(4.25), is important. Though not yet well studied, a mesophase can appear in near-critical binary mixtures with addition of such salt.³⁰

(iv) To describe ionic surfactants, we have presented the amphiphilic interaction F_{am} in Eq.(2.13) characterized by the parameter w_a and the rod length 2ℓ . As Fig. 7-9 demonstrate, F_{am} serves to induce adsorption of ionic surfactants onto an interface reducing the surface tension γ , which becomes significant for large w_a . In our 1D calculations in Fig. 9, γ decreases to zero with increasing the surfactant density or the parameter w_a . In real 3D systems,¹⁸ micells are formed from the interface beyond a critical surfactant density before vanishing of γ . In addition, we are neglecting the steric effect due to the finite size of the surfactant molecules.

(v) In one-phase states of near-critical mixtures, a peak can appear at an intermediate wave number in the structure factor of the composition fluctuations for $\gamma_p > 1$, where $\gamma_p (\propto g_1 - g_2)$ defined by Eq.(3.5) is the parameter representing the solvation asymmetry. Below the transition, a mesoscopic phase can emerge, as observed recently.³⁰ It can occur for strongly asymmetric salt (say, salt composed of hydrophilic cations and hydrophobic anions).³ It should be induced more easily for ionic surfactants, as Eq.(3.5) indicates.

(vi) We have derived the attractive interactions among ions mediated by the critical fluctuations as in Eq.(3.11). We should then investigate how they can produce large-scale structures near the criticality.^{34,35} It is also of interest how charged colloidal particles interact in polar fluids in the presence of strong solvation effects.

(vii) To understand the experiment,³⁶ we have examined the situation where three ion species are present. As shown in Fig. 5, the ion distributions around an interface can be much more complex than in the case of two ion species.

We mention future problems.

(1) There can be an electric double layer and a potential difference at an interface in general charged systems, including polymers, surfactant systems, and gels. Results on the structure factor in Section 3 can be used

for polymer solutions and blends. The solvation coupling between the ion densities and the composition should generally be present in such systems. From the viewpoint of the solvation effects, as delineated in this chapter, more experiments with addition of ions are informative in soft matters.

(2) We have assumed mild heterogeneity of the dielectric constant of a mixture. However, it can be very strong in aqueous mixtures including polymeric systems. For example, we may assume $\epsilon_A \sim 100$ and $\epsilon_B \sim 1$. We have not yet understood electric field effects in such extreme (but common) situations.

(3) The steric effect due to a finite volume fraction of ionic surfactants becomes crucial with increasing its density, leading to saturation of the adsorption onto an interface, though it has been neglected in this chapter. We will soon report on this effect.

(4) Wetting should be greatly influenced by ions. Wetting on colloid surfaces can give rise to attraction among colloids.³⁷ If the wetting layer is more polar than the outer fluid, ions can even be confined within the layer.³⁸

(5) Phase separation in ionic systems should also be investigated. Ions are more strongly segregated than the fluid components for large g_i . We already examined the effect of a very small amount of ions on nucleation.⁹

(6) Ion dynamics near an interface is also intriguing, when ionic surfactants are present or when electric field is applied.

(7) We examined solvation effects of charged particles in liquid crystals.³⁹ In nematic states the dielectric tensor anisotropically depends on the director orientation and ions distorts the orientation order over long distances and sometimes create manometer scale defects.

References

1. J. N. Israelachvili, *Intermolecular and Surface Forces* (Academic Press, London, 1991).
2. Y. Marcus, *Ion Solvation* (Wiley, New York, 1985).
3. A. Onuki and H. Kitamura, *J. Chem. Phys.* **121**, 3143 (2004).
4. A. Onuki, *Phys. Rev. E* **73**, 021506 (2006).
5. M. Born, *Z. Phys.* **1**, 45 (1920).
6. Le Quoc Hung, *J. Electroanal. Chem.* **115**, 159 (1980); *ibid.* **149**, 1 (1983).
7. T. Osakai and K. Ebina, *J. Phys. Chem. B* **102**, 5691 (1998).
8. J.J. Thomson, *Conduction of Electricity through Gases* (Cambridge University Press, Cambridge, 1906), Sec.92.
9. H. Kitamura and A. Onuki, *J. Chem. Phys.* **123**, 124513 (2005).
10. C. Wagner, *Phys. Z.* **25**, 474 (1924).
11. L. Onsager and N. N. T. Samaras, *J. Chem. Phys.* **2**, 528 (1934).

12. Y. Levin and J. E. Flores-Mena, *Europhys. Lett.* **56**, 187 (2001).
13. G. Jones and W. A. Ray, *J. Am. Chem. Soc.* **59**, 187 (1937); *ibid.* **63**, 288 (1941); *ibid.* **63**, 3262 (1941).
14. N. Matubayasi, H. Matsuo, K. Yamamoto, S. Yamaguchi, and A. Matuzawa, *J. Colloid Interface Sci.* **209**, 398 (1999).
15. P. B. Petersen and R. J. Saykally, *J. Am. Chem. Soc.* **127**, 15446 (2005).
16. M. Manciu and E. Ruckenstein, *Adn. Colloid Interface Sci.* **105**, 10468 (2003).
17. J. D. Reid, O. R. Melroy, and R.P. Buck, *J. Electroanal. Chem.* **147**, 71 (1983).
18. S.A. Safran, *Statistical Thermodynamics of Surfaces, Interfaces, and Membranes* (Westview Press, 2003).
19. J.E. Guyer, W.J. Boettinger, J.A. Warren, G.B. McFadden, *Phys. Rev. E* **69**, 021603 (2004); *ibid.* **69**, 021604 (2004).
20. Y. Tsori and L. Leibler, *Proceedings of the National Academy of Sciences of the United States of America* **104**, 7348 (2007).
21. A. Onuki, *Phase Transition Dynamics* (Cambridge University Press, Cambridge, 2002).
22. P. Debye and K. Kleboth, *J. Chem. Phys.* **42**, 3155 (1965).
23. M. Laradji, H. Guo, M. Grant, and M. Zukermann, *J. Phys. A* **24**, L629 (1991).
24. J. Traube, *Ann. Chem. Liebigs.* **265**, 27 (1891).
25. J.W. Gibbs, *Collected works*, vol.1, pp.219-331 (1957), New Haven, CT: Yale University Press.
26. E.L. Eckfeldt and W.W. Lucasse, *J. Phys. Chem.* **47**, 164 (1943).
27. B.J. Hales, G.L. Bertrand, and L.G. Hepler, *J. Phys. Chem.* **70**, 3970 (1966).
28. V. Balevicius and H. Fuess, *Phys. Chem. Chem. Phys.* **1**, 1507 (1999).
29. V.M. Nabutovskii, N.A. Nemov, and Yu.G. Peisakhovich, *Phys. Lett. A*, **79**, 98 (1980); *Sov. Phys. JETP* **52**, 111 (1980) [*Zh.Eksp.Teor.Fiz.* **79**, 2196 (1980)].
30. K. Sadakane, H. Seto, H. Endo, and M. Shibayama, *J. Phys. Soc. Jpn.*, **76**, 113602 (2007).
31. V. Yu. Boryu and I. Ya. Erukhimovich, *Macromolecules* **21**, 3240 (1988).
32. J.F. Joanny and L. Leibler, *J. Phys. (France)* **51**, 545 (1990).
33. I.F. Hakim and J. Lal, *Europhys. Lett.* **64**, 204 (2003).
34. J. Jacob, M.A. Anisimov, J.V. Sengers, A. Oleinikova, H. Weingärtner, and A. Kumar, *Phys. Chem. Chem. Phys.* **3**, 829 (2001).
35. A. F. Kostko, M. A. Anisimov, and J. V. Sengers, *Phys. Rev. E* **70**, 026118 (2004).
36. G. Luo, S. Malkova, J. Yoon, D. G. Schultz, B. Lin, M. Meron, I. Benjamin, P. Vanysek, and M. L. Schlossman, *Science*, **311**, 216 (2006).
37. D. Beysens and T. Narayanan, *J. Stat. Phys.* **95**, 997 (1999).
38. N.A. Denesyuk and J.-P. Hansen, *J. Chem. Phys.* **121**, 3613 (2004).
39. A. Onuki, *J. Phys. Soc. Jpn.* **73**, 511 (2004).